

A study of top quark pair production in association with a high energy photon at the LHC

Thuso Mathaha¹, Abhaya Kumar Swain¹, Bruce Mellado^{1,2}

¹School of Physics and Institute for Collider Particle Physics, University of the Witwatersrand, Johannesburg, Wits 2050, South Africa

²iThemba LABS, National Research Foundation, PO Box 722, Somerset West 7129, South Africa

E-mail: 1144845@students.wits.ac.za

Abstract. We conducted a study of the ratio of the top quark pair in association with a photon to the top quark pair at the precision of NLO QCD predictions at the LHC with the top quark decay leptonically. This channel is selected because it provides a clean signal while limiting all the background contamination. The top quark pair production cross-section has been measured at LO and NLO in proton-proton collisions at $\sqrt{s} = 13$ TeV. The events with exactly one electron and one muon, at least two jets, one of which is a b-tagged, are selected. Monte Carlo simulations at leading-order and next-to-leading-order accuracy are used to construct many relevant kinematic observables. These observables are the kinematic variables involving the photon, the angular separation between the two leptons, and the angular separation between the photon and leptons etc.

1. Introduction

With a mass m_t that is significantly higher than any of the other quark and that is very close to the scale at which electroweak symmetry breaks, the top quark is the heaviest known fundamental particle. A crucial element of the Large Hadron Collider (LHC) physics program is the study of its production and decay characteristics. Top quarks are primarily produced at the LHC in quark-antiquark pairs ($t\bar{t}$), and the precise prediction of the corresponding inclusive cross-section is dependent on both the top quark mass and the gluon parton distribution function (PDF). This poses a significant challenge for QCD calculational methods. The rate at which the top quark pair is produced can be enhanced in physics beyond the standard model. For evaluating the predictions of the Standard Model (SM) and its potential extensions, precise measurements of top-quark production are needed. Since its mass is at electroweak scale and in order to understand its electroweak interaction, the production of top-quark pair associated with a high-energy photon can be used to explore the $t\gamma$ electroweak coupling. Additionally, the measurements of the cross-sections of these processes are particularly important since these topologies are delicate to physics beyond the SM (BSM). Thus the purpose of this study can be broken into two parts, first is to provide a systematic analysis in the dilepton top quark decay channel for both processes; $pp \rightarrow t\bar{t}$ and $pp \rightarrow t\bar{t}\gamma$, while we aim to find the most detailed NLO prediction for the cross section ratio. The second part is looking at potential correlations between the two processes in different regions of phase space in an effort to reduce any theoretical

mistakes, it will be feasible to determine whether differential cross section ratios have improved predictive capacity for new physics searches.

2. Event selection

The ATLAS and CMS experiments at the LHC are actively driving top quark studies, which are crucial for understanding the basic interactions. The top quarks are dominantly produced in pairs at the LHC through strong interactions, although they can also be produced individually by electroweak interactions. The top quark therefore enables various testing of the underlying forces depending on the production mode. The measurements of top quark parameters, such as top quark mass, width, charge, total and differential cross sections, top quark spin correlations, and top quark charge asymmetry, including differential top quark charge asymmetries, are the main focus of both experiments.

The final state topologies in the top-quark pair production are reliant on the decay modes of the W bosons since the top quark decays 99.8% of the time in the SM to a W boson and a b -quark [1]. The channel with two leptons (electron and muon pair) with opposite electric charges referred to as $e\mu$ channel and is considered a clean signal because it contains less background contamination. This channel has been utilized to provide the most accurate ATLAS measurements of top-quark pair cross section at center of mass energy $\sqrt{s} = 7, 8$ and 13 TeV [2, 3, 4], based on events with an opposite-sign $e\mu$ pair and one or two b -tagged jets. The CDF Collaboration presented the first evidence for the production of $t\bar{t}$ in association with a high energy photon ($t\bar{t}\gamma$) and the ATLAS Collaboration confirmed the process' observation in proton-proton collisions at $\sqrt{s} = 7$ TeV [5]. The top pair cross-section was measured by the ATLAS and CMS Collaborations at $\sqrt{s} = 8$ TeV [6, 7]. The ATLAS Collaboration made the first measurements of the inclusive and differential cross sections at $\sqrt{s} = 13$ TeV [8]. In the final state with one electron and one muon, the fiducial inclusive and differential combined $t\bar{t} + t\bar{t}\gamma$ production cross-sections have been measured and are presented in this study. We also took into consideration instances where the electrons and muons emerge from the leptonic decays of tau-leptons as part of our signal in order to further investigate the multilepton anomalies. As a function of photon kinematic factors, angular variables associated to the photon and the leptons, and angular separations between the two leptons in the event, the absolute differential cross-sections are measured in the fiducial area.

The differential distributions of the leptons generated in $t\bar{t}$ events may also be precisely measured using the $e\mu + b$ -tagged jet sample. At $\sqrt{s} = 8$ TeV, ATLAS has previously reported measurements of the absolute and normalized differential cross-sections as functions of the transverse momentum p_T^l ($l = e, \mu$) and absolute pseudorapidity $|\eta^l|$ of the single leptons, the $p_T^{e\mu}$, invariant mass $m_{e\mu}$ and absolute rapidity $|y^{e\mu}|$ of the $e\mu$ system, the absolute azimuthal angle $|\Delta\phi|$ amongst the two leptons in the transverse direction, not forgetting the scalar sum of the momentum of leptons and their respective energies. These distributions were found to be typically well represented by predictions from a range of next-to-leading order (NLO) fixed-order QCD computations and leading order (LO) multileg. It was also shown that the results were sensitive to both the top quark pole mass and the gluon PDF. Using $t\bar{t}$ and $t\bar{t}\gamma$ samples that are roughly six times as large as those available at $\sqrt{s} = 8$ TeV, in this study we measure the same distributions at the increased center of mass energy of $\sqrt{s} = 13$ TeV. The results of several LO matrix-element event generators are again compared to the NLO matrix-element events for both $t\bar{t}$ and $t\bar{t}\gamma$.

The reason for selecting the $e\mu$ channel is because of its clean final state with minor background contamination and the lack of requiring multivariate analysis technique to separate the signal and background processes. In order to compare the cross-sections with the theoretical

calculation in Ref. [8], the cross-sections are also measured at the parton level rather than the particle level. The calculation represents the first comprehensive computation for $t\bar{t}$ production with and without a hard final-state photon in hadronic collisions at NLO, taking into account all resonant and non-resonant diagrams, interferences, and off-shell effects of the top quarks and the W bosons.

3. Monte Carlo simulation

The Monte Carlo (MC) event generator was used to model the events for the signal processes that we are interested in using madgraph5 [9], and Delphes [10] was utilized to mimic the response of the ATLAS detector. Using the NNPDF2.3LO PDF [11] set of settings, Pythia 8 [12] was utilized to produce more pp interactions that crossed through or were adjacent to bunch crossing. The two signals were produced independently at matrix-element level with and without a photon at both the LO and NLO in QCD.

The ATLAS detector was utilized to collect the 139 fb^{-1} of integrated luminosity data that were used in this analysis during the period of Run 2. The main physics objects taken into account in this study are photons, jets, b -jets, missing transverse momentum, and leptons in the form of electrons and muons. With the assistance of reconstructed tracks in the ID system, the energy deposits in the electromagnetic calorimeter are used to reconstruct the electrons. They are chosen using a tight working point from a combined likelihood approach [13], and they must be separated based on the calorimeter and tracking quantities. If an electron meets $|\eta| < 2.5 \text{ GeV}$ and $p_T > 25 \text{ GeV}$, it is chosen. Muons are reconstructed using an algorithm that integrates the track segments from the muon spectrometer and the ID tracks. The isolation criteria of the muon in the track and calorimeter is similar to the one applied to the electrons. While the track must start from the primary collision vertex, muons that satisfy $|\eta| < 2.5$ and $p_T > 25 \text{ GeV}$ are chosen.

Energy accumulated at the electromagnetic calorimeter's core is used to reconstruct photons. If the candidates match one or two reconstructed tracks that are compatible with coming from a photon conversion, they are chosen. The selection requirements are met by photons with $p_T > 25 \text{ GeV}$ and $|\eta| < 2.37$. Their energies are calibrated in Ref. [14], and they are reconstructed and recognized as described there. The anti- k_t algorithm is used to the topological cluster of cells in the calorimeter to reconstruct jets [15] with a distance $\Delta R \leq 0.4$ [16]. The selected jets need to have $p_T > 25 \text{ GeV}$ and $|\eta| < 2.5$. By using the b -tagging algorithm (MV2c10) to the jets, b -quark hadronization jets known as b -jets are detected. The track impact parameters and secondary vertices are used in this approach, which is based on a boosted decision tree. The selection criteria for both signal processes employed in this study are the same, except for $t\bar{t}\gamma$ there is an extra requirement; events must contain at least one photon that meets the aforementioned photon criterion. By contrasting distributions, the modeling of the signal processing at LO and NLO is examined. Figure 1 displays a number of kinematic characteristics that are significant to this investigation.

4. Results

At the center-of-mass energy of $\sqrt{s} = 13 \text{ TeV}$ for Run II of the LHC, the distributions for the $pp \rightarrow t\bar{t}$ and $pp \rightarrow t\bar{t}\gamma$ processes were determined. Finding the dominant partonic subprocesses is useful for determining the correlations and any differences between the two production processes. The scattering of two gluons is the primary source of energy in both cases, and the gg channel contributes the majority 79% (88%)—of the LO $pp \rightarrow t\bar{t}$ ($pp \rightarrow t\bar{t}\gamma$) cross section, while the $q\bar{q}+q\bar{q}$ channels make up only a small portion—21% (12%) [17]. The kinematics of the final states in $pp \rightarrow t\bar{t}$ and $pp \rightarrow t\bar{t}\gamma$, with two charged leptons, their transverse momentum, and b -tagged

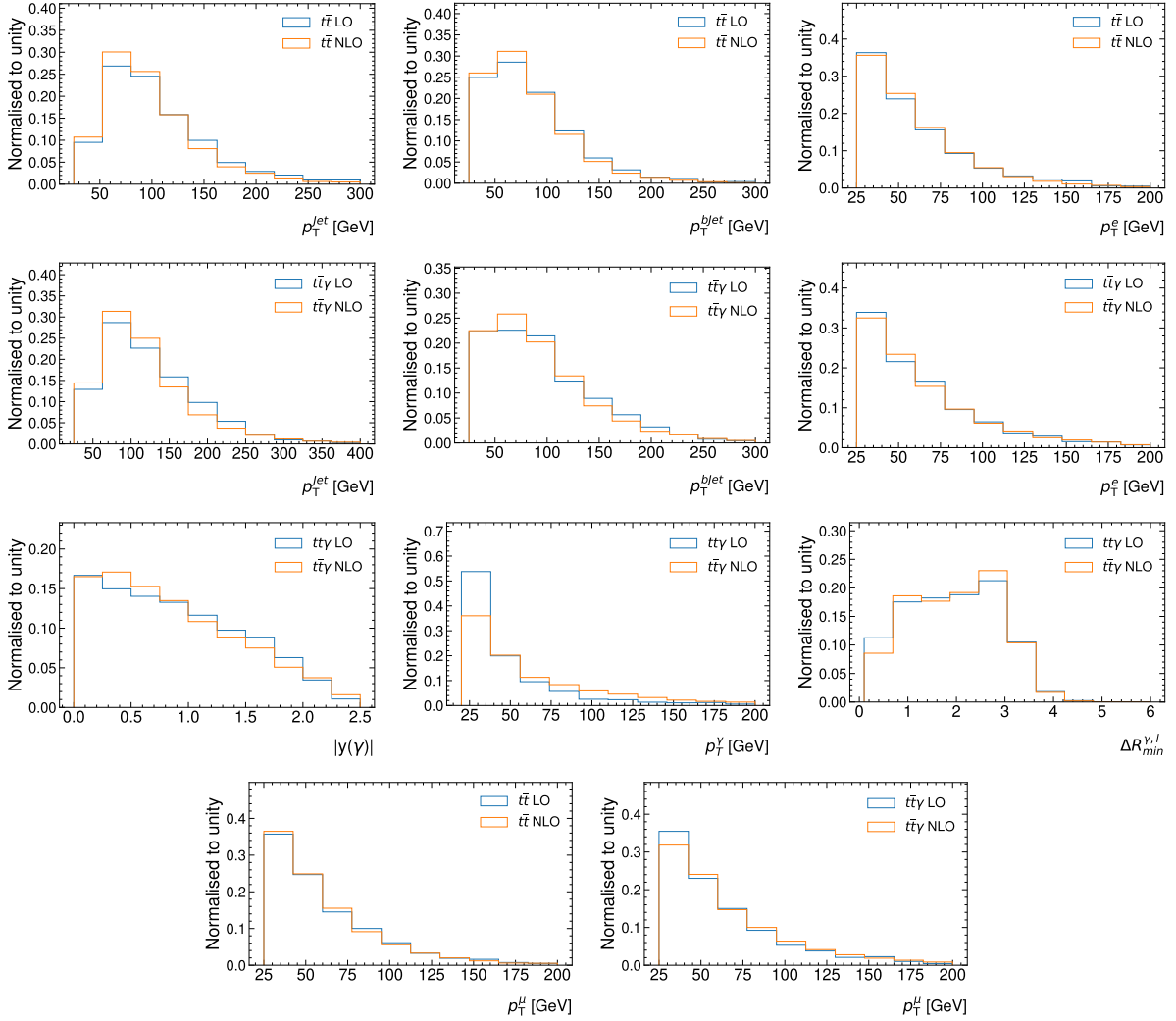


Figure 1. Distributions of the transverse momentum of jets, b -jets, the electron for $t\bar{t}$ ($t\bar{t}\gamma$) signal in the 1st (2nd) row. The 3rd row is the rapidity of the photon, transverse momentum of the photon and the separation in the rapidity-azimuthal angle plane between a photon and a lepton for $t\bar{t}\gamma$. The transverse momentum of the muon for signals is in the bottom row. The LO distributions are in blue while the NLO distributions are in orange.

jets, should be similar due to the domination of the gg production process in both instances. The NNPDF23 set has been utilized for all of the differential cross sections that are shown in the following. For both production processes, we use the kinematic-independent factorization and renormalization scales $\mu_R = \mu_F = \mu_0$ with the central value m_t since both processes are comparable from the perspective of QCD, as indicated by the kinematic distributions in figure 1. The transverse momentum of the b jets, the two leptons, and the transverse momentum of the jets for both processes have previously been collected. In order to highlight shape similarities and differences between the two processes, the distributions are normalized to unity. The distributions do not significantly change between the two processes although in some kinematic variables we do see change. This is because gg production predominates, favoring jet emissions at slower rates [17].

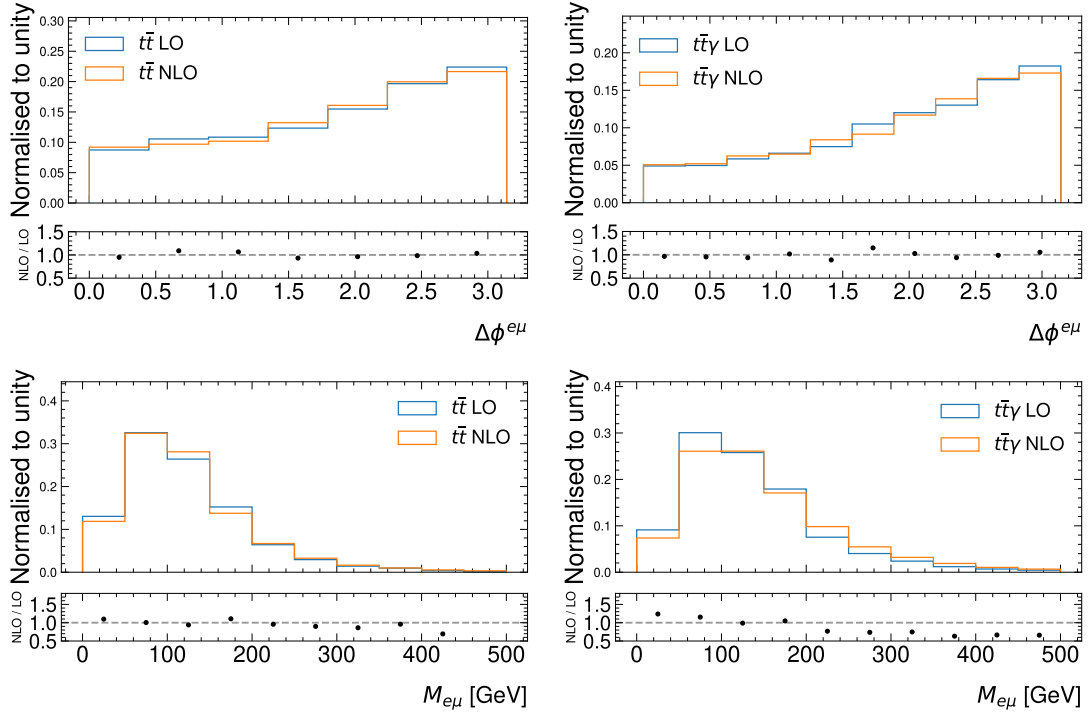


Figure 2. Distributions of $\Delta\phi^{e\mu}$ in the top row and the invariant mass of the two leptons in the bottom row. They are also accompanied by the ratio plots of NLO to LO distributions.

4.1. Ratio of cross sections

Our main goal is to see if there is any way to make theoretical forecasts even more accurately. We also wish to examine about whether theoretical uncertainties rely on certain fixed scales. The cross-section ratio equations (Eqn 1 and 2) will be used to describe a quantity in order to look for deviations from the standard model theory at the LHC.

$$\mathfrak{R}_{LO} = \frac{\sigma_{t\bar{t}\gamma}}{\sigma_{t\bar{t}}} = \frac{0.2298}{59.9} = 0.0038 \quad (1)$$

$$\mathfrak{R}_{NLO} = \frac{\sigma_{t\bar{t}\gamma}}{\sigma_{t\bar{t}}} = \frac{0.2489}{76.54} = 0.0033 \quad (2)$$

To be more precise, we want to see if the theoretical uncertainties for the fixed scale choice can be maintained to around 10%. On the other hand, we would want to examine if a few percent precision, or accuracy similar to that of NNLO calculations for $t\bar{t}$ production, can be attained in the case of the dynamical scale choice used in this study. From an experimental standpoint, measurements in the regions of phase space defined by particular selection cuts that closely mimic detector response are more appropriate, simply because such measurements do not introduce unnecessary extra uncertainties due to model-dependent extrapolations to parton level $t\bar{t}$ objects and to regions of phase space outside the detector sensitivity. Reduced final state decay products paired with hard photon emission from charged leptons and b-jets drastically alter the ratio. Figure 2 displays the ratio of NLO to LO as a function of the azimuthal angle shift in the $e\mu$ channel and the invariant mass of two leptons. According to the ratio plots in Fig. 2, the products at LO and NLO do not differ much from one another, with the exception of higher momentum values, particularly for the invariant masses of the two charged leptons.

5. Conclusion

The main objective of this work is to get more accurate theoretical predictions for top quark pair $t\bar{t}$ production in the di-lepton channel. In order to achieve this, meaningful cross-section ratios for $t\bar{t}$ and $t\bar{t}\gamma$ production have been investigated using completely realistic NLO simulations. They are based on LO and NLO matrix components for the $2\rightarrow 6$ and $2\rightarrow 7$ production processes, which contain interference for all top quark and W boson interactions. It has been looked at how the cross-section ratio is affected by different renormalization and factorization scale options as well as parton distribution functions. Our most accurate NLO QCD predictions for the R observable have been made using the NNPDF3.0 pdf collection. Other pdf sets can be examined in future research to enhance the cross-section outcomes, which might enhance the discrepancy between the two processes.

References

- [1] Tanabashi M, Hagiwara K and Hikasa K (Particle Data Group) 2018 *Phys. Rev. D* **98**(3) 030001 URL <https://link.aps.org/doi/10.1103/PhysRevD.98.030001>
- [2] Collaboration A *et al.* 2014 *arXiv preprint arXiv:1406.5375*
- [3] Collaboration A 2016 *Eur. Phys. J. C* **76** 642
- [4] Avdeeva E, Bartek R, Dominguez A, Fangmeier C, Gonzalez Suarez R, Kamalieddin R, Kravchenko I, Malta Rodrigues A, Meier F, Monroy J *et al.* 2017
- [5] Aad G, Abbott B, Abdallah J, Khalek S A, Aben R, Abi B, Abolins M, AbouZeid O, Abramowicz H, Abreu H *et al.* 2015 *Physical review D* **91** 072007
- [6] Demir D A, Collaboration C *et al.* 2011 *European Physical Journal C*
- [7] Aguilar-Saavedra J A 2018 *The European Physical Journal C* **78** 1–8
- [8] Berlendis S, Cheu E, Delitzsch C, Johns K, Jones S, Lampl W, LeBlanc M, Leone R, Loch P, Nayyar R *et al.* 2019
- [9] Alwall J, Herquet M, Maltoni F, Mattelaer O and Stelzer T 2011 *Journal of High Energy Physics* **2011** 1–40
- [10] De Favereau J, Delaere C, Demin P, Giammanco A, Lemaitre V, Mertens A and Selvaggi M 2014 *Journal of High Energy Physics* **2014** 1–26
- [11] Pumplin J, Stump D R, Huston J, Lai H L, Nadolsky P and Tung W K 2002 *Journal of High Energy Physics* **2002** 012
- [12] Sjöstrand T, Ask S, Christiansen J R, Corke R, Desai N, Ilten P, Mrenna S, Prestel S, Rasmussen C O and Skands P Z 2015 *Computer physics communications* **191** 159–177
- [13] collaboration A *et al.* 2011 *arXiv preprint arXiv:1110.3174*
- [14] Aad G, Aggarwal A, Caron S, Colasurdo L, Fabiani V, Gottardo C, Ilic N, Konig A, Pedraza Diaz L and Schouwenberg J 2019
- [15] Collaboration A *et al.* 2015 Properties of jets and inputs to jet reconstruction and calibration with the atlas detector using proton–proton collisions at $\sqrt{s}=13$ tev Tech. rep. ATL-PHYS-PUB-2015-036
- [16] Cacciari M, Salam G P and Soyez G 2008 *Journal of High Energy Physics* **2008** 063
- [17] Bevilacqua G, Hartanto H, Kraus M, Weber T and Worek M 2019 *Journal of High Energy Physics* **2019** 1–29